Dispersion Behaviors of Copper Oxide on the Mixed "$CeO_2 + \gamma$-Al_2O_3" Support

L. Dong,* Y. Hu, M. Shen, T. Jin, J. Wang, W. Ding, and Y. Chen

Department of Chemistry, Laboratory of Mesoscopic Materials and Chemistry, Nanjing University, Nanjing, 210093, China

Received October 24, 2000. Revised Manuscript Received August 8, 2001

The dispersion behaviors of copper oxide on the mechanical mixture of CeO_2 and γ-Al_2O_3 supports, $CuO/CeO_2 + \gamma$-Al_2O_3, have been characterized by using XRD, LRS, XPS, UV-DRS, and TPR. The results show that copper oxide dispersed mainly on the surface of CeO_2 support, provided that the loading amount of copper oxide does not exceed the dispersion capacity of CuO/CeO_2, ~1.2 mmol of CuO/100 m^2 of CeO_2 (Dong, L.; Jin, Y. S.; Chen, Y. *Sci. China (B).* **1997**, *40*, 24). Increasing the CuO loading evidently leads to the formation of the dispersed copper oxide species on the surface of the γ-Al_2O_3 support. The results have been tentatively discussed by using the incorporation model, which was proposed to describe the interaction between the dispersed species and the support previously (Chen, Y.; Zhang, L. F. *Catal. Lett.* **1992**, *12*, 51).

1. Introduction

In recent years, mixed oxides (designated as A−B), such as CeO_2–ZrO_2,[1−3] TiO_2–SiO_2,[4] SiO_2–Al_2O_3,[5−6] and TiO_2–Al_2O_3,[7−9] have been extensively studied for their potential applications as the supports in catalyst preparations. These materials not only take advantage of both A and B but also extend their applications through the generation of new catalytic active sites due to the interaction of A with B. For example, ceria−zirconia materials have oxygen-storage and oxygen-buffering capacities, high thermal stability, and large surfaces area and have been regarded as potential catalysts for environmental catalysis;[2,3] titania−silica materials have shown the properties of an n-type semiconductor and an active catalytic support, with high thermal stability and excellent mechanical strength, and have been extensively studied for application in photocatalysis, acid catalysis, etc.[4] For all the mixed oxide materials, generally, they are mainly prepared by using coprecipitation, sol−gel, impregnation, and precipitation methods, etc. During the past years, a lot of physicochemical characterization methods, such as XRD, XPS, TEM, IR, Raman, TPR, TPO, and TPD, have been used to study these systems to get a deeper understanding about the nature of the systems. However, due to the complexity of the composition and the interactions among the components in these systems,[1−9] the real roles of the components and the states of them in the mixed oxide support are difficult to clarify. For example, CeO_2–ZrO_2 prepared by the coprecipitation method may include a Ce−Zr−O solid solution, CeO_2-modified ZrO_2 crystalline (CeO_2/ZrO_2), and ZrO_2-modified CeO_2 crystalline (ZrO_2/CeO_2), as well as the mixture of ZrO_2 and CeO_2 crystallines. When this material is used for a support to prepare a catalyst, e.g. CuO/CeO_2–ZrO_2, the interaction among the supports and copper oxide will be quite complex.

As known to all, ceria, as an active component, has been widely used for TWC (three-way catalysis) applications because of its remarkable redox properties. The capacity of ceria to store and release oxygen enables the car exhaust purification catalyst to operate more efficiently by making it less sensitive to the continuous lean/rich oscillations occurring in the exhaust stream.[10] Copper oxide has been demonstrated to be a very active species among the base-metal oxides as oxidation catalysts, in which the catalysts based upon $CuO-Al_2O_3$ oxides have been used in a variety of processes in chemical industry,[11] and in recent years, it has been studied as a substitute for automotive postcombustion.[12]

As reported previously,[13−15] the copper oxide can disperse on the surfaces of CeO_2 and γ-Al_2O_3 to form

* Corresponding author. E-mail: chem718@netra.nju.edu.cn.

(1) Arias, A. M.; Garcia, M. F.; Belver, C.; Conesa, J. C.; Soria, J. *Catal. Lett.* **2000**, *65*, 197.
(2) Fally, F.; Perrichchon, V.; Vidal, H.; Kaspar, J.; Blanco, G.; Pintado, J. M.; Bernal, S.; Colon, G.; Daturi, M.; Lavalley, J. C. *Catal. Today.* **2000**, *59*, 373.
(3) Ozaki, T.; Masui, T.; Machida, K.; Adachi, G.; Sakata, T.; Mori, H. *Chem. Mater.* **2000**, *12*, 643.
(4) Davis, R. J.; Liu, Z. F. *Chem. Mater.* **1997**, *9*, 2311.
(5) Yoshida, H.; Kato, Y.; Hattori, T. *Stud. Surf. Sci. Catal.* **2000**, *130*, 659.
(6) Koningsberger, D. C.; Oudenhuijzen, M. K.; Ramaker, D. E.; Miller, J. T. *Stud. Surf. Sci. Catal.* **2000**, *130*, 317.
(7) Powell, Q. H.; Fotou, G. P.; Kodas, T. T.; Anderson, B. M. *Chem. Mater.* **1997**, *9*, 685.
(8) Klimova, T.; Ramirez, J.; Cuevas, R.; Gonzalez, H. *Stud. Surf. Sci. Catal.* **2000**, *130*, 2801.
(9) Cedeno, L.; Zanella, R.; Ramirez, J.; Lopez Agudo, A. *Stud. Surf. Sci. Catal.* **2000**, *130*, 2807.
(10) Taylor, K. C. In *Proceeding of First International Symposium on Catalysis and Automotive pollution Control*; Brussels, 1986.
(11) Knozinger, H. *Adv. Catal.* **1976**, *25*, 184.
(12) Lin, P. Y.; Skoglundh, M.; Lowendahl, L.; Dahl, J. E.; Jansson, K.; Nygren, M. *Appl. Catal. B-Env.* **1995**, *6*, 237.
(13) Dong, L.; Hu, Y. H.; Xu, F.; Lu, D.; Xu, B.; Hu, Z.; Chen, Y. *J. Phys. Chem.* **2000**, *104*, 78.
(14) Chen, Y.; Dong, L.; Jin, Y.; Xu, B.; Ji, W. *Stud. Surf. Sci. Catal.* **1996**, *101*, 1293.
(15) Hu, Y. H.; Dong, L.; Wang, J.; Ding, W. P.; Chen, Y. *J. Mol. Catal. (A, Chem.)* **2000**, *162*, 307.

10.1021/cm0008462 CCC: $20.00
Published on Web 10/23/2001

the supported catalysts CuO/CeO_2 and $CuO/\gamma\text{-}Al_2O_3$, respectively. In the present work, the attention is mainly focused on the study of the dispersion behaviors of copper oxide species on the mixed CeO_2 and $\gamma\text{-}Al_2O_3$ support by monitoring the relationship between the changes of the properties of the dispersed copper oxide and the loading amount of copper oxide. This method is expected to explore the influencing factors for the dispersion of copper oxide on CeO_2 and $\gamma\text{-}Al_2O_3$. For this purpose, a mechanical mixture of "$CeO_2 + \gamma\text{-}Al_2O_3$" has been used as the support, and the $CuO/CeO_2 + \gamma\text{-}Al_2O_3$ system has been taken to study the interactions among the copper oxide and the mixture supports. The results show that the interactions between the copper oxide and CeO_2 and $\gamma\text{-}Al_2O_3$ are quite different: copper oxide mainly disperses on the surface of ceria while the copper loading is less than the dispersion capacity (~1.2 mmol of CuO/100 m^2 of CeO_2)[14,15] of the CuO/CeO_2 system.

2. Experimental Section

Samples. $\gamma\text{-}Al_2O_3$ support was purchased from Fusun Petrochemical Institute of China, and the BET surface area was 216 $m^2.g^{-1}$ after precalcination in air at 700 °C for 5 h. CeO_2 support was prepared by calcining $Ce(NO_3)_3{\cdot}6H_2O$ in air at 550 °C for 5 h, and the BET surface area was 55 $m^2.g^{-1}$.

Mixed "$CeO_2 + \gamma\text{-}Al_2O_3$" support was prepared by fully grinding a mixture of $\gamma\text{-}Al_2O_3$ and CeO_2 support, in which the weight-ratio of $CeO_2/\gamma\text{-}Al_2O_3$ was 4/1. In this case, the surface area of CeO_2 support is close to that of $\gamma\text{-}Al_2O_3$ in the mixture.

The copper oxide supported catalysts were prepared by the incipient wetness impregnation of "$CeO_2 + \gamma\text{-}Al_2O_3$" support with an aqueous solution containing the requisite amount of $Cu(NO_3)_2$, and the wet samples were dried in air at 100 °C for 12 h and then calcined in a flowing O_2 stream at 450 °C for 5 h.

Instruments. XRD (X-ray diffraction) patterns were obtained with a Shimadzu XD-3A diffractometer employing Cu Kα radiation (0.15418 nm), and the X-ray tube was operated at 35 kV and 20 mA.

BET surface areas were measured by nitrogen adsorption at 77 K on a Micrometrics ASAP-2000 adsorption apparatus.

FT-Raman spectra were recorded on a Bruker RFS-100 spectrometer with an InGaAs detector cooled by liquid nitrogen. Raman excitation at 1064 nm was provided by a Na:YAG laser. The laser power measured at the sample (~30 mg) was 100 mW, and spectra were accumulated for 50 scans at 4 cm^{-1} resolution in backscattering geometry.

XPS (X-ray photoelectroscopy spectra) were recorded with a V. G. Escalab MK II system equipped with a hemispherical electron analyzer. The spectrometer was operated at 15 kV and 20 mA, and a magnesium anode (Mg Kα = 1253.6 eV) was used. Al2p1/2(74.5 eV) was taken as a reference to calculate the binding energies (BE).

UV-DRS (UV−visible diffuse reflectance spectra) was recorded in the range of 200−700 nm by a Shimadzu UV-2100 spectrometer with $BaSO_4$ as reference.

TPR (temperature-programmed reduction) was carried out in a quartz U-tube reactor, and 30 mg catalyst was used for each measurement. Prior to the reduction, the catalyst was pretreated in a N_2 stream at 100 °C for 1 h and then cooled to room temperature. After that an H_2–Ar mixture (7% H_2 by volume) was switched on the system. The temperature was increased linearly at a rate of 10 °C min^{-1}.

3. Results and Discussion

Dispersion of Copper Oxide on the Mixed Support. The BET surface area of the mixed "$CeO_2 + \gamma\text{-}Al_2O_3$" support is 86.2 $m^2.g^{-1}$, and the deposition of copper oxide causes a decreasing surface area, from 86.2 to 74.4 $m^2.g^{-1}$. For the $CuO/CeO_2 + \gamma\text{-}Al_2O_3$ samples (noted as CuCeAlXX, in which XX represents the CuO loading), the data are shown as in Table 1. However, the surface areas of the samples were almost unchanged (about 74.8 $m^2.g^{-1}$) as CuO loadings were increased from 0.9 to 2.0 mmol/100 m^2 of CeO_2, which suggested that the surface of the mixed support was not evidently varied during the preparation procedure and implied that the copper oxide mainly existed as highly dispersed species on the surface of the support. Figure 1 shows the XRD results of $CuO/CeO_2 + \gamma\text{-}Al_2O_3$ samples with CuO loadings varying from 0.1 to 3.0 mmol/100 m^2 of CeO_2. In XRD patterns, four diffraction peaks centering at about $2\theta = 28.3°$, 33.2°, 47.6°, and 57.1° are observed, which correspond to the diffraction of the CeO_2 support. The diffraction peak(s) corresponding to the $\gamma\text{-}Al_2O_3$ support is not observed, probably due to the relative lower sensitivity of γ-alumina as compared to ceria. For the samples a−g, there are no detectable diffraction peaks representing crystalline CuO in the samples, even if CuO loadings are increased to 2.0 mmol/100 m^2 of CeO_2, suggesting that the copper oxide species have been highly dispersed on the surface of the mixed support. However, the diffraction peaks corresponding to crystalline CuO, at $2\theta = 35.5°$ and 38.7°, are shown in pattern h, which indicates the formation of crystalline CuO due to the high copper loading.

Table 1. BET Surface Areas of $CuO/CeO_2 + \gamma\text{-}Al_2O_3$ Samples with Different CuO Loading

samples	CuO loadings[a] (mmol/100 m^2 of CeO_2)	BET areas (m^2/g)
CuCeAl00	0	86.2
CuCeAl01	0.1	79.1
CuCeAl09	0.9	74.4
CuCeAl12	1.2	71.1
CuCeAl18	1.8	74.8
CuCeAl20	2.0	74.8

[a] The CuO loading, XX mmol of CuO/100 m^2 of CeO_2, is calculated according to the surface area of CeO_2 in the sample.

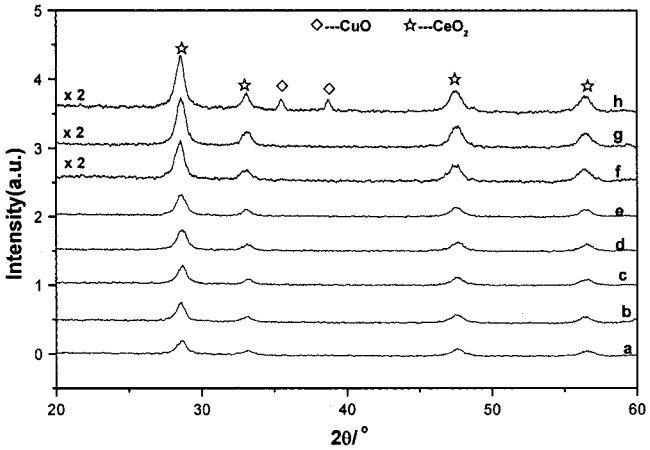

Figure 1. XRD patterns of $CuO/CeO_2 + \gamma\text{-}Al_2O_3$ samples a, b, c, d, e, f, g, and h with loading amounts of CuO of 0.1, 0.3, 0.6, 0.9, 1.2, 1.8, 2.0, and 3.0 mmol/100 m^2 of CeO_2, respectively.

Raman spectra of $CuO/CeO_2 + \gamma\text{-}Al_2O_3$ samples are shown in Figure 2. For the lower CuO-loaded samples, e.g., 0.1 and 0.3 mmol/100 m^2 of CeO_2, the spectra a and b show a strong Raman band at about 462 cm^{-1} and another weaker one at about 250 cm^{-1}, which have been attributed to the contribution of the CeO_2 surface

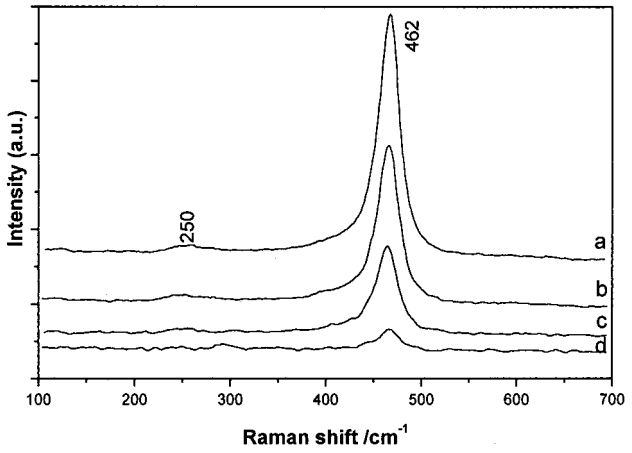

Figure 2. Raman results of $CuO/CeO_2 + \gamma\text{-}Al_2O_3$ samples a, b, c, and d with loading amounts of CuO of 0.1, 0.3, 0.6, and 0.9 mmol/100 m^2 of CeO_2, respectively.

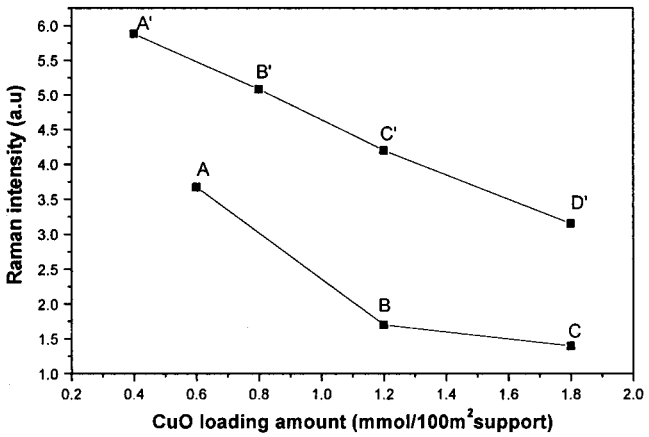

Figure 3. Raman band intensity of the CeO_2 at 462 cm^{-1} as a function of CuO loading in various samples: line A′D′ corresponds to the "CeO_2 + $CuO/\gamma\text{-}Al_2O_3$" system, and line AC corresponds to the "$CuO/CeO_2 + \gamma\text{-}Al_2O_3$" system.

due to the F_{2g} Raman active mode characteristic of fluorite structure materials.[16] Noticeable, it has shown that the addition of copper oxide results in the dramatically decreased Raman intensity of the CeO_2 support. From 0.1 to 0.9 mmol/100 m^2 of CeO_2, the greater the amount of CuO loaded, the weaker the Raman band becomes, as shown in spectra a−d. Although it is a fact that the samples with copper oxide loaded are colored, which can induce heating effects influencing the Raman intensity,[17] it seems reasonable to suggest that the decreased Raman intensity of CeO_2 in the mixed support is strongly related to the coverage of the CeO_2 surface by the dispersed copper oxide species. To approach this suggestion, a relationship between the Raman intensity variation and the copper contents is shown in Figure 3. For "$CuO/CeO_2 + \gamma\text{-}Al_2O_3$" and "$CeO_2$ + $CuO/\gamma\text{-}Al_2O_3$" systems, increasing the copper loading leads to the decrease of the Raman intensity in both of the series samples. The results mean that the Raman vibration signal of the CeO_2 support has been decreased, whether the copper oxide covers the surface of the CeO_2 support or exists as copper oxides (such as crystalline CuO and $CuO/\gamma\text{-}Al_2O_3$) in the CeO_2 support. However, for the same copper oxide loading, the dispersed copper oxide on the surface of CeO_2 has a stronger influence on the Raman signal than the crystalline copper oxide powder or $CuO/\gamma\text{-}Al_2O_3$ does. For "CeO_2 + $CuO/\gamma\text{-}Al_2O_3$" samples, the Raman intensity decreased almost in a straight line as the copper loading increased, but the decrease of the Raman intensity in "$CuO/CeO_2 + \gamma\text{-}Al_2O_3$" samples could be seen as the organization of two lines with different slopes. The turn-point appeared to correspond to the dispersion capacity of CuO/CeO_2, ∼1.2 mmol of CuO/100 m^2 of CeO_2. In the $CuO/CeO_2 + \gamma\text{-}Al_2O_3$ system, the results indicate that the Raman intensity in line AB decreases more strongly than that in line BC, which should mainly correspond to the influences of the coverage of copper oxide on ceria and the dilution effect of ceria by the contained copper oxide materials (such as $CuO/\gamma\text{-}Al_2O_3$), respectively. Furthermore, these results imply that the dispersion capacity of a metal oxide species on a support could be determined by monitoring the change of the surface properties of the support, such as the surface M═O Raman vibration intensity of MO_x. Likewise, in some other systems,[18−20] the dispersion of copper oxide, vanadium, and molybdenum oxide species on metal oxide supports has also been reported to cause a dramatic decrease in the intensity of the Raman bands from the metal oxide supports.

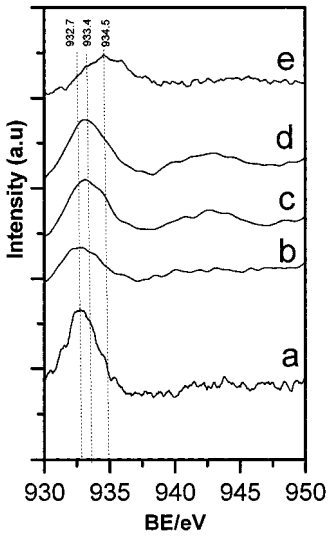

Figure 4. XPS results of various supported copper oxide samples: (a) CuO/CeO_2 samples with CuO loading of 0.3 mmol/100 m^2 of CeO_2; (b, c, and d) "$CuO/CeO_2 + \gamma\text{-}Al_2O_3$" samples with CuO loading of 0.6, 1.2, and 1.8 mmol/100 m^2 of CeO_2, respectively; and (e) $CuO/\gamma\text{-}Al_2O_3$ sample with CuO loading of 0.1 mmol/100 m^2 of $\gamma\text{-}Al_2O_3$.

Figure 4 shows the XPS results of $CuO/CeO_2 + \gamma\text{-}Al_2O_3$ samples with different copper oxide contents. As a reference, the XP spectra of CuO/CeO_2 and $CuO/\gamma\text{-}Al_2O_3$ are displayed, too. For the variation of the copper loadings from 0.6 to 1.8 mmol of CuO/100 m^2 of CeO_2, the BE values varied from 932.6 to 933.2 eV. Considering that the binding energies of copper oxide in CuO/CeO_2 and $CuO/\gamma\text{-}Al_2O_3$ are 932.7 and 934.5 eV, respectively, as shown in spectra a and e, the shift of the BE values, from 932.6 to 933.2 eV, should be

(16) Kermidas V. G.; White, W. B. *J. Phys. Chem.* **1973**, *59*, 1561.
(17) Mestaland, G.; Knozinger, H. In *Handbook of Heterogeneous Catalysis*; VCH: Weinheim, 1997; Vol. 2.
(18) Larsson, P. O.; Andersson, A.; Wallenberg, L. R.; Svensson, B. *J. Catal.* **1996**, *163*, 279.
(19) Larsson, P. O.; Andersson, A. *J. Catal.* **1998**, *179*, 72.
(20) Busca, G.; Zecchina, A. *Catal. Today* **1994**, *20*, 61.

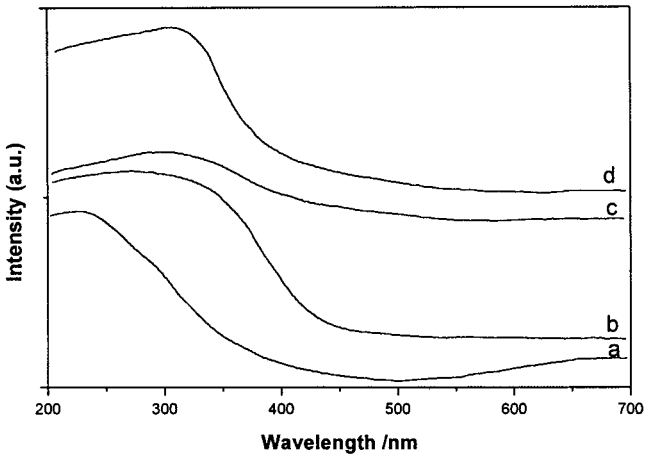

Figure 5. UV-DRS results of various CuO supported catalysts: (a) CuO/γ-Al_2O_3 catalyst with a loading amount of CuO 0.3 mmol/100 m^2 of γ-Al_2O_3, (b) CeO_2 support, (c and d) CuO/CeO_2 catalysts with loading amounts of CuO of 0.6 and 1.2 mmol/100 m^2 of CeO_2, respectively.

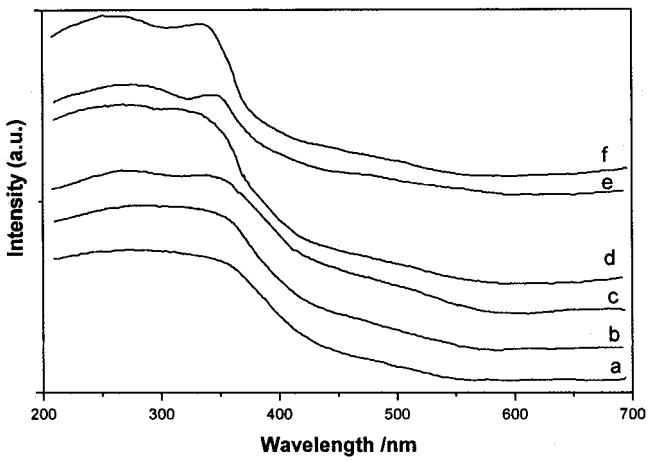

Figure 6. UV-DRS results of CuO/CeO_2 + γ-Al_2O_3 samples a, b, c, d, e, and f with loading amounts of CuO of 0.3, 0.6, 0.9, 1.2, 1.8,and 2.0 mmol/100 m^2 of CeO_2, respectively.

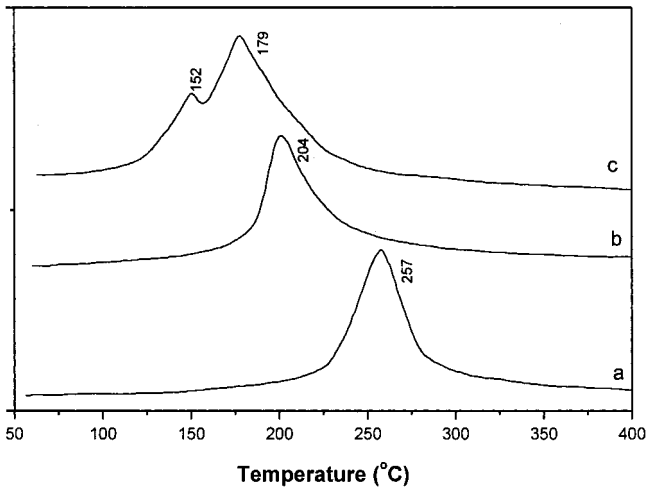

Figure 7. TPR profiles of different CuO-containing samples: (a) CuO and (b) CuO/γ-Al_2O_3 sample with a loading amount of CuO of 0.3 mmol/100 m^2 of γ-Al_2O_3, and (c) CuO/CeO_2 sample with a loading amount of CuO of 0.6 mmol/100 m^2 of CeO_2, respectively.

ascribed to the contribution of the coexistence of dispersed CuO on both CeO_2 and γ-Al_2O_3 in the CuO/CeO_2 + γ-Al_2O_3 system due to the copper loading beyond the dispersion capacity of CuO/CeO_2, ~1.2 mmol of CuO/100 m^2 of CeO_2. The results are basically in agreement with that of XRD; e.g., no detectable XRD peaks of crystalline CuO could be shown in XRD patterns for the samples containing the same copper loadings.

To approach the properties of the dispersed copper species on the mixture support "CeO_2 + γ-Al_2O_3", as for the references, the UV-DRS results for a copper oxide respectively supported on CeO_2 and γ-Al_2O_3 are shown in Figure 5. For the CuO/γ-Al_2O_3 sample, the absorption band of surface-dispersed copper oxide species is around 250 nm, while for the CuO/CeO_2 sample, the absorption band appears at about 320 nm for the surface-dispersed copper oxide species, which is different from that observed in the CuO/γ-Al_2O_3 sample. The results suggest that the properties of the surface-dispersed copper oxide are extensively influenced by the supports,[21] and it is possible to distinguish the dispersed copper species formed on CeO_2 and/or γ-Al_2O_3 support.

The UV-DRS results of CuO/CeO_2 + γ-Al_2O_3 samples with different CuO loadings are shown in Figure 6. For the samples (Figure 6a−c) with CuO loadings of 0.3−0.9 mmol/100 m^2 of CeO_2, the spectra are similar to the spectrum in Figure 5c, in which the absorption band is corresponding to the dispersed copper species on CeO_2. As CuO loadings are increased to ≥1.2 mmol/100 m^2 of CeO_2, the absorption band at 320 nm becomes stronger, and another band at about 250 nm is also obviously observed simultaneously, as shown in spectra d−f. The results mean that, with the addition of the copper oxide exceeding the dispersion capacity of copper oxide on CeO_2, the evident formation of the dispersed copper oxide on the surface of γ-Al_2O_3 occurs besides the dispersion of copper oxide on CeO_2 surface.

TPR profiles of CuO/CeO_2 and CuO/γ-Al_2O_3 samples are shown in Figure 7, and the reduction profile of CuO powder is also presented for comparison. For CuO and CuO/γ-Al_2O_3 samples, TPR curves a and b show a single peak of maximum hydrogen consumption at about 257 and 204 °C, respectively. While for the CuO/CeO_2 sample (curve c), the TPR profile shows two peaks of hydrogen consumption maxima at 152 and 179 °C, respectively, which has been discussed elsewhere.[15] It is worth noting that the reduction temperatures in the present studies are lower than that reported in ref 15, this decrease is presumably due to the higher heating rate and gas flow rate as well as the treatments.[22] Figure 8 shows the TPR curves of CuO/CeO_2 + γ-Al_2O_3 samples with different CuO loadings. The shapes of TPR profiles change significantly as CuO loadings are increased. For the samples a, b, and c with CuO loadings <1.2 mmol/100 m^2 of CeO_2, there are two peaks with hydrogen consumption maxima at about 151 and 182 °C, respectively, and the peak intensities are also increased with CuO loadings from 0.3 to 0.9 mmol/100 m^2 of CeO_2. For the samples with CuO loadings ≥1.2 mmol/100 m^2 of CeO_2, another peak at about 205 °C is observed besides the peaks at 151 and 182 °C. Compar-

(21) Kobayashi, H.; Takezawa, N.; Shimokawabe, M.; Takahashi, K. *Stud. Surf. Sci. Catal.* **1983**, *16*, 697.

(22) Shyu, J. Z.; Weber, W. H.; Gandhi, H. S. *J. Phys. Chem.* **1988**, *92*, 4964.

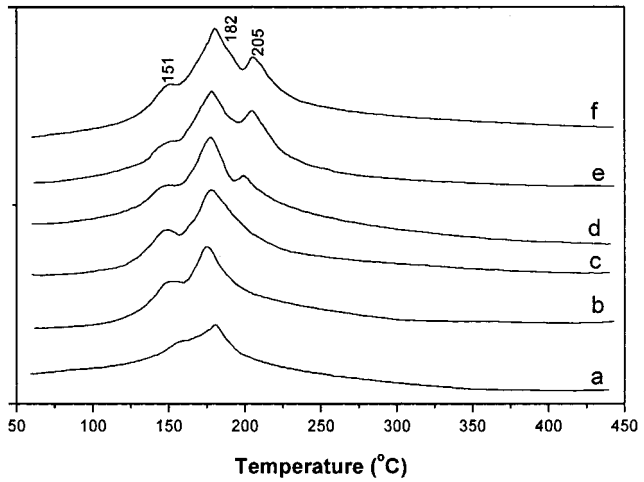

Figure 8. TPR profiles of $CuO/CeO_2 + \gamma\text{-}Al_2O_3$ samples a, b, c, d, e, and f with loading amounts of CuO of 0.3, 0.6, 0.9, 1.2, 1.8, and 2.0 mmol/100 m^2 of CeO_2, respectively.

ing the above results with those in Figure 7, it seems to suggest that the peaks at 151 and 182 °C should be ascribed to the reduction of the dispersed copper oxide on CeO_2 and the peak at 205 °C is due to the reduction of surface-dispersed copper oxide species on $\gamma\text{-}Al_2O_3$ support, as well as no evident formation of crystalline CuO in the samples. All the TPR results are in agreement with those obtained by XRD, LRS, and UV-DRS.

A Tentative Explanation for the Preferential Dispersion of Copper Oxide on the Surface of Ceria. It is well-known[14,17,23,24] that the dispersion of metal oxides on the oxide supports is extensively influenced by the surface structure of the support and other factors, such as preparation methods, the calcination temperature, and calcination atmosphere. In this study, we mainly discuss the possible causes that lead to the preferential dispersion of copper oxide on the surface of CeO_2 rather than the $\gamma\text{-}Al_2O_3$ support by considering the differences of the surface structures of the supports.

In the mixed support, CeO_2 and $\gamma\text{-}Al_2O_3$ almost have the same surface areas; generally, the copper oxide has the same opportunity to disperse on both of the supports. However, the results show that the copper oxide species have a preferential dispersion on the surface of the CeO_2 support when the loading amount of CuO did not exceed its dispersion capacity on ceria.

As reported elsewhere, for the $NiO/\gamma\text{-}Al_2O_3$ and $MoO_3/\gamma\text{-}Al_2O_3$ systems with a relatively lower loading amount of the active components,[25−29] Ni^{2+} and Mo^{6+} ions preferentially incorporate into the surface tetrahedral vacancies rather than the octahedral ones on the surface of $\gamma\text{-}Al_2O_3$ after a calcination at about 450 °C. Considering the mixture support with (111) and (110) planes

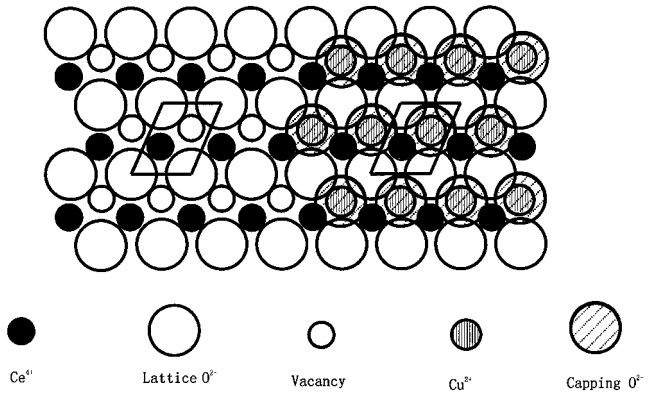

Figure 9. The schematic diagram for the incorporated Cu^{2+} ions in the surface vacant site of the CeO_2 (111) plane.

being preferentially exposed on CeO_2[30,31] and $\gamma\text{-}Al_2O_3$,[32−33] respectively, tetrahedral and octahedral vacancies exist on the surface of $\gamma\text{-}Al_2O_3$, and the cubic vacancies exist on the surface of CeO_2. Generally speaking, the surface lattice oxygen of the support shows some different properties as compared with the bulk lattice oxygen; e.g, it is coordination unsaturated. Recently, it has been shown by the spectral characterization that the coordination-unsaturated surface lattice oxygen ions have an abnormal tendency to donate electrons.[34,35] It is well-known that the most important role for ceria, during the catalysis process, is to store and release oxygen under, respectively, lean and rich conditions.[10] The surface lattice oxygen ions are active in the surface reactions, as has been suggested by a recent atomic simulation of a carbon monoxide oxidation mechanism on cerium oxide[36] and from which it could be deduced that the surface lattice oxygen ions on CeO_2 are relatively more active than those on $\gamma\text{-}Al_2O_3$. This unique characteristic of ceria seems to suggest that the preferential dispersion of copper oxide on the surface of ceria should be related to an intrinsic surface property. In addition, Cu^{2+} ion is $3d^94s^0$ and has only one unpaired electron, and there are stronger covalent contributions in the Cu−O bond of dispersed copper oxide species.[37] Consequently, the incorporated Cu^{2+} ions might have a stronger interaction with the surrounding surface lattice oxygen of CeO_2 than they have with $\gamma\text{-}Al_2O_3$, as has been observed in the TPR results on the ceria-supported copper oxide species with a lower reduction temperature. For the $CuO/CeO_2 + \gamma\text{-}Al_2O_3$ system, copper oxides can disperse on each support and incorporate in the vacancies on the supports. However, on the basis of our results, the copper ions preferentially incorporated in the cubic vacancies on ceria, and the surface structure of the dispersed copper oxide species could be deduced by consideration of the incorporation model,[29] as shown in Figure 9.

(23) Knozinger, H.; Taglauer, E. In *Catalysis*; Royal Society of Chemistry: London, 1993; Vol. 10.
(24) Wachs, I. E. *Catal. Today* **1996**, *27*, 437.
(25) Lo Jacono, M.; Schvavello, M.; Cimino, A. *J. Phys. Chem*. **1971**, *75*, 1044.
(26) Wu, M.; Hercules, D. M. *J. Phys. Chem*. **1979**, *83*, 2003.
(27) Burggaf, L. W.; Leyden, D. E.; Chin, R. L.; Hercules, D. M. *J. Catal*. **1982**, *78*, 360.
(28) Chen, Y.; Zhang, L. F.; Lin, J. F.; Jin. Y. S. *Catal. Sci. Technol*. **1991**, *1*, 291.
(29) Chen, Y.; Zhang, L. F. *Catal. Lett*. **1992**, *12*, 51.
(30) Cochrane, H. D.; Hutchison, J. L. *Ultramicroscopy* **1989**, *31*, 138.
(31) Dong, L.; Chen. Y. *J. Chem. Soc., Faraday Trans*. **1996**, *92*, 4589.
(32) Beaufils, P.; Barbaux, Y. *J. Chim. Phys*. **1981**, *78*, 347.
(33) Jimenez-Conzalez, J.; Schmeiber, D. *Surf. Sci*. **1991**, *250*, 59.
(34) Tench, A. J.; Nelson, R. L. *Trans. Faraday Soc*. **1967**, *63*, 2254.
(35) Che, M.; Naccache, C.; Imelik, B. *J. Catal*. **1972**, *24*, 328.
(36) Seyle, T. X. T.; Parker, S. C.; Catlow, C. R. A. *J. Chem. Soc., Chem. Commun*. **1992**, 997.
(37) Xia, W. S.; Wan, H. L.; Chen, Y. *J. Mol. Catal., A* **1999**, *138*, 185.

4. Conclusions

LRS, XPS, UV-DRS, and TPR results indicate that, in $CuO/CeO_2 + \gamma\text{-}Al_2O_3$ samples, copper oxide species have a preferential dispersion on the surface of the CeO_2 support, which suggests that the extent of interaction between copper oxide and CeO_2 and $\gamma\text{-}Al_2O_3$ is different. The preferential dispersion of copper oxide on ceria could be related to the intrinsic surface properties of ceria.

Acknowledgment. The financial support of the Special Foundation for the Doctor-subject of China (No. 98028434) is gratefully acknowledged.

CM0008462